Research Article Vol. 37, No. 1 / January 2020 / Journal of the Optical Society of America A 149

Journal of the Optical Society of America A

OPTICS, IMAGE SCIENCE, AND VISION

Analytic design of a spherochromatic singlet

RAFAEL G. GONZÁLEZ-ACUÑA* AND JULIO C. GUTIÉRREZ-VEGA

Photonics and Mathematical Optics Group, Tecnológico de Monterrey, Monterrey 64849, Mexico
**Corresponding author: rafael.guillermo.ga@gmail.com*

Received 5 September 2019; revised 2 December 2019; accepted 2 December 2019; posted 3 December 2019 (Doc. ID 377075); published 20 December 2019

We derive the analytic formula of the output surface of a spherochromatic lens. The analytic solution ensures that all the rays for a wide range of wavelengths fall inside the Airy disk. So, its amount of spherical aberration is small enough to consider the lens as diffracted limited. We test the singlet lens using ray-tracing methods and find satisfactory results, including spot diagram analysis for three different Abbe wavelengths.

https://doi.org/10.1364/JOSAA.37.000149

1. INTRODUCTION

A spherochromatic singlet is a lens designed to reduce spherical and chromatic aberration. Traditionally, achromatic lenses are built with two or three lenses paired together [1–3]. This paradigm began in the 18th century with Isaac Newton's claim that correcting chromatic aberration with a singlet lens was impossible [4]. Mainly because of this belief, Newton focused on designing telescopes with mirrors instead of lenses [4,5]. Actually, the problem is much more ancient and can be traced back to two centuries BC when the Greek mathematician Diocles first proposed a parabolic mirror to collect a bundle of rays as a manner to emulate the effect of a single lens [6]. Renowned scientists resumed the problem of designing achromatic lenses with minimal spherical dispersion. For example, Christiaan Huygens wrote in the preface of his classical optics book, *Traité de la lumiére* [7], that Newton and Leibniz were interested in knowing the shape of a lens such as it collects the light, quoting: "*I have meditated the things which now I publish, and not for the purpose of detracting from the merit of those who, without having seen anything that I have written, may be found to have treated of like matters: as has in fact occurred to two eminent Geometricians, Messieurs Newton and Leibniz, with respect to the Problem of the figure of glasses for collecting rays when one of the surfaces is given.*" Huygens tried on his own to find the analytic shape of the lens with zero aberration and failed in the attempt by joining other famous mathematicians who also tried, such as Newton and Descartes. Huygens in the sixth chapter of *Traité de la lumiére* proposed a numerical solution to the problem for a single wavelength, but he did not find any expression for more than one wavelength [7,8]. The first achromatic doublet was developed by Chester Moore Hall in 1729, and soon later, in 1758, John Dollond registered the first patent of a doublet lens [5,9]. Recently, the problem of finding a singlet free of spherical aberration was mathematically solved and reported in Ref. [10] for a single wavelength.

The same paradigm is still present today, namely, the doublets and triplets are traditionally the basic elements to reduce chromatic aberration in an optical system [2,3]. The standard approach consists of optimizing numerically the system parameters to minimize spherochromatic aberration. These numerical approaches are very useful for particular applications, but they do not provide mathematically rigorous solutions [11–13]. Recently, an optimization-based method was proposed for the design of apochromatic singlet lenses with negative refraction indices under the paraxial approximation [14].

In this paper, we derive a powerful closed-form analytic equation to design the surface of a spherochromatic singlet lens. In the process of deriving the expression, we introduce a formal and fully analytic approach for design singlets free of spherical and chromatic aberration [10,15–17]. We test the singlet lens using accurate ray-tracing methods and find very satisfactory results for spot diagram analysis for three different Abbe wavelenghts.

2. MATHEMATICAL MODEL

The geometry of the singlet is shown in Fig. 1. We assume that the lens is a rotationally symmetric element with axial thickness t surrounded by air. We locate the origin of the coordinate system just at the first surface whose shape is flat, and it is described by the function $z_a(r_a) = 0$, where sub-index a refers to the coordinates on the input surface. The output surface is described by the unknown function $z_b(r_b)$, where sub-index b refers to the coordinates at the output surface.

A polychromatic source point (O) in a steady state is placed on-axis at $z = t_a$ from the input surface. The image point (I) is located beyond the lens at an axial distance t_b from the output surface, as shown in Fig. 1. The material dispersion of the glass

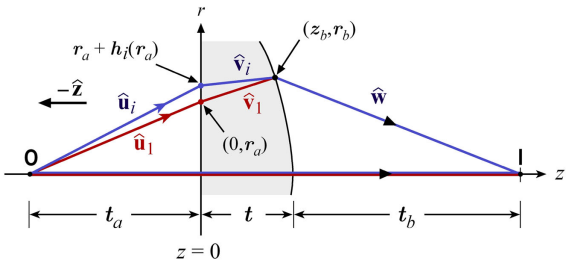

Fig. 1. Meridional half-plane of the spherochromatic singlet, illustrating the deviation of the incoming rays by the surfaces and their optical paths traversed. For clarity, we show only two rays, but the analysis is general for any number of wavelengths, and thus we use the notation h_i for the i-th ray.

is characterized by the variation of the refractive index versus the wavelength $n(\lambda)$. Although our analysis is general for many wavelengths, for definiteness, we will characterize the glass according to the usual practice of giving the refractive index at three particular wavelengths, e.g., the Abbe wavelengths, so $n(\lambda_i) = n_i$ for $i \in \{1, 2, 3\}$.

The goal is to determine the function $z_b(r_b)$ of the output surface in order to eliminate the spherical and chromatic aberration at the image point (I). This means that rays emerging from the source point with different angles and wavelengths converge exactly on the image point after they have been refracted by the lens. Note that the direction of the rays traveling along the optical axis is not affected by the lens independently of their wavelengths, so they automatically meet the condition.

For off-axis rays, consider three rays with different propagation angles and wavelengths $(\lambda_1, \lambda_2, \lambda_3)$ impinging on the lens. For clarity, in Fig. 1, we show only two rays. The first ray (in red) strikes the lens at point $(0, r_a)$, and it is considered as the reference ray; the propagation unit vectors as it passes through the segments of air–glass–air are denoted by $\hat{\mathbf{u}}_1$, $\hat{\mathbf{v}}_1$, $\hat{\mathbf{w}}$, respectively. A second ray (in blue) is selected in such a way that it hits the input surface at a radial separation $h_2(r_a)$ from the first ray and emerges from the lens just at the same point as the reference ray does and with the same wavevector b $\hat{f}w$. In this way, both rays arrive at the image point with the same propagation angle. The distance $h_2(r_a)$ is *a priori* unknown and should be determined in the process. In general, for a ray with wavelength λ_i, the separation between its input point on the first surface with respect to the reference ray (λ_1) will be denoted as $h_i(r_a)$, and thus, $h_1 = 0$.

The hypothesis of this work is that there must be an analytic function $z_b(r_b)$ for the output surface that ensures that two rays with different angles and wavelengths satisfy the condition of reaching the image point (I) with the same inclination, i.e., the same slope. If this is true for two rays with arbitrary angles and wavelengths, then by extension, it going to be true for three, four, and more rays with arbitrary angles and wavelengths.

To begin the analysis, we will first derive the condition to ensure that the system is free of spherical aberration. Consider that the source (O) emits simultaneously two rays with the same wavelength λ_i; the first one travels along the optical axis z, and the second one strikes the input surface of the singlet at $(0, r_a + h_i)$. Both rays pass through the singlet and meet again at the image point (I) located at $z = t + t_b$. The Fermat principle requires that the optical lengths between points (O) and (I) be the same for both ray trajectories. Thus, equating the optical paths, we get the following set of algebraic equations for the unknowns z_b, r_b, h_i:

$$-t_a + n_i t + t_b = \sqrt{(r_a + h_i)^2 + t_a^2} + n_i\sqrt{z_b^2 + (r_b - r_a - h_i)^2} + \sqrt{r_b^2 + (z_b - t - t_b)^2}, \tag{1}$$

where for each wavelength, $i \in \{1, 2, 3\}$, and where $h_1 = 0$. We remark that Eq. (1) represents actually three different relations, and each one must be satisfied separately. That is, the optical path length (OPL) for all the rays with the same wavelength is equal, but the OPL for rays with different wavelengths is different.

The parameters of the ray with λ_i are further related through the application of the Snell law at the first surface. Let

$$-\hat{\mathbf{z}} = [-1, 0] \tag{2a}$$

be the normal vector of the input surface pointing toward the incident medium, and

$$\hat{\mathbf{u}}_i = \frac{[t_a, r_a + h_i]}{\sqrt{(r_a + h_i)^2 + t_a^2}}, \tag{2b}$$

$$\hat{\mathbf{v}}_i = \frac{[z_b, r_b - r_a - h_i]}{\sqrt{(r_b - r_a - h_i)^2 + z_b^2}} \tag{2c}$$

be the propagation unit vectors of the incident and refracted rays, respectively (see Fig. 1). The Snell law relating these vectors reads in vector form as follows:

$$\hat{\mathbf{v}}_i = \frac{\hat{\mathbf{z}}}{n_i} \times (\hat{\mathbf{z}} \times \hat{\mathbf{u}}_i) + \frac{\hat{\mathbf{z}}}{n_i}\sqrt{n_i^2 - |\hat{\mathbf{u}}_i \times \hat{\mathbf{z}}|^2}. \tag{3}$$

Substituting Eq. (2) into (3) and separating the components, we get the following expressions for the direction cosines of the vector $\hat{\mathbf{v}}_i$:

$$\mathcal{R}_i \equiv \frac{r_b - r_a - h_i}{\sqrt{(r_b - r_a - h_i)^2 + z_b^2}} = \frac{r_a + h_i}{n_i\sqrt{(r_a + h_i)^2 + t_a^2}}, \tag{4a}$$

$$\mathcal{Z}_i \equiv \frac{z_b}{\sqrt{(r_b - r_a - h_i)^2 + z_b^2}} = \sqrt{1 - \frac{(r_a + h_i)^2}{n_i^2[(r_a + h_i)^2 + t_a^2]}}, \tag{4b}$$

where $\mathcal{R}_i^2 + \mathcal{Z}_i^2 = 1$, and $i \in \{1, 2, 3\}$.

Equations (1) and (4) form a system of nonlinear algebraic equations for the unknowns z_b, r_b, and h_i that apparently do not have a closed analytical solution. Fortunately, we have found that under the approximation $|h_i| \ll |r_b - r_a|$, the numerator in the left-hand side of Eq. (4a) reduces to $(r_b - r_a)$, and the resulting nonlinear system can be solved analytically. This approximation is physically valid by virtue of the small variation

in the refraction index with respect to the wavelength. The exact solution of the simplified system of nonlinear equations is given by

$$z_b = \frac{\mathcal{Z}_1\sqrt{AB + C} + D}{A}, \tag{5a}$$

$$r_b = r_a + \frac{\mathcal{R}_1 z_b}{\mathcal{Z}_1}, \tag{5b}$$

$$h_i = \frac{n_i^2\mathcal{R}_1^2 t_a^2}{n_i\mathcal{R}_1 t_a\sqrt{\mathcal{Z}_1^2 - (n_i^2 - 1)\mathcal{R}_1^2}} - r_a, \tag{5c}$$

with the special value $h_1 = 0$, and where

$$A \equiv \mathcal{Z}_1^2\left[9 - \left(\sum_{i=1}^{3}\frac{n_i}{\mathcal{Z}_i}\right)^2\right] + 9\mathcal{R}_1^2, \tag{6a}$$

$$B \equiv (F - 3t_b - 3t)\,(F + 3t_b + 3t) - 9r_a^2, \tag{6b}$$

$$C \equiv \left\{\mathcal{Z}_1\left[F\sum_{i=1}^{3}\frac{n_i}{\mathcal{Z}_i} - 9(t_b + t)\right] + 9\mathcal{R}_1 r_a\right\}^2, \tag{6c}$$

$$D \equiv 9\mathcal{Z}_1[\mathcal{Z}_1(t_b + t) - \mathcal{R}_1 r_a] - F\mathcal{Z}_1^2\sum_{i=1}^{3}\frac{n_i}{\mathcal{Z}_i}, \tag{6d}$$

$$F \equiv t\sum_{i=1}^{3} n_i + 3t_b - \left(3t_a - \sum_{i=1}^{3}\sqrt{(r_a + h_i)^2 + t_a^2}\right). \tag{6e}$$

The system of Eqs. (1) and (4) and its simplified analytic solution (5) constitute the most important result of this work. They express in an analytic closed form the shape of the output surface of a dispersive singlet free of spherical and chromatic aberration and whose refractive index is characterized with three wavelengths (λ_1, λ_2, λ_3). The surface is described in parametric form with the functions $z_b(r_a)$ and $r_b(r_a)$, where r_a plays the role of an independent radial variable. These expressions may look cumbersome, but it is quite remarkable that the output shape may be expressed in closed algebraic form. We have restricted the analysis to three wavelengths, but the method can be straightforwardly extended to more wavelengths. To the best of our knowledge, this expression has not been obtained before. Equation (5) specifies the shape of the singlet under the approximation $|h_i| \ll |r_b - r_a|$ that, as we will see later, is physically valid for typical values in realistic applications. Finally, we remark that Eq. (5) is valid when all the refraction indices are positive for each wavelength and, moreover when all are negative for each wavelength as well. So, the relations may be applied to devices built with metamaterials.

3. ILLUSTRATIVE EXAMPLE

To test our model, we solved numerically the exact nonlinear system of Eqs. (1) and (4) and compared the solution with the simplified result given by the analytic expression in Eq. (5). Let us consider a spherochromatic singlet

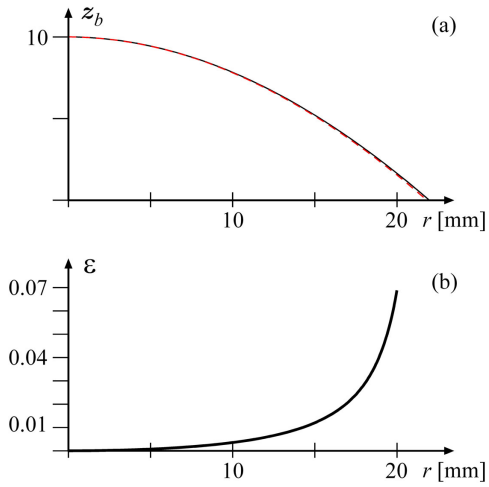

Fig. 2. (a) Surface of the singlet $z_b(r_b)$ for the parameters given in the text. Solid black line is the numeric solution of the exact system of Eqs. (1) and (4). Dashed red line is the plot of the analytic solution (5). (b) Percentage error between both solutions.

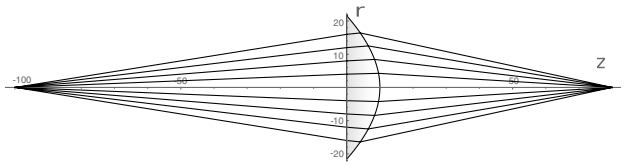

Fig. 3. Ray diagram of a spherochromatic singlet lens for light with $\lambda_1 = 587.6$ nm. The ray trajectories for λ_2 and λ_3 have been omitted because they practically overlap with rays with λ_1, making it difficult to visualize. Geometrical parameters are included within the text.

built with BK7 glass with refractive indices $n_1 = 1.5168$, $n_2 = 1.5224$, and $n_3 = 1.5143$, corresponding to the wavelengths $\lambda_1 = 587.6$ nm, $\lambda_2 = 486.1$ nm, and $\lambda_3 = 656.3$ nm, respectively. We have chosen arbitrarily the object distance $t_a = -100$ mm, lens axial thickness $t = 10$ mm, and image distance $t_b = 70$ mm.

In Fig. 2(a), we plot the output surface $z_b(r_b)$ predicted by the exact system (black curve) and the simplified analytic model (dashed red curve). We evaluated 500 points, and the differences between both surfaces were lower than 10^{-6} mm. The percentage error defined as

$$\varepsilon = \frac{|\text{Exact} - \text{Approx}|}{|\text{Exact}|} \times 100\% \tag{7}$$

between both solutions is plotted in Fig. 2(b), where we can conclude that both curves are quite similar.

The tracing of the rays with wavelength λ_1 is depicted in Fig. 3 for the singlet specified above. For this selection of refractive indices, the values of h_i are small, e.g., for $r_a = 5$ mm, we get $h_1 = 0$, $h_2 = 0.10$ mm, and $h_3 = 0.08$ mm. In view of this, it is not practical to show graphically the ray trajectories for two or three wavelengths, because they practically overlap in the plot.

To have a qualitative way to evaluate the efficiency of the system and to compare with a monochromatic diffraction-free

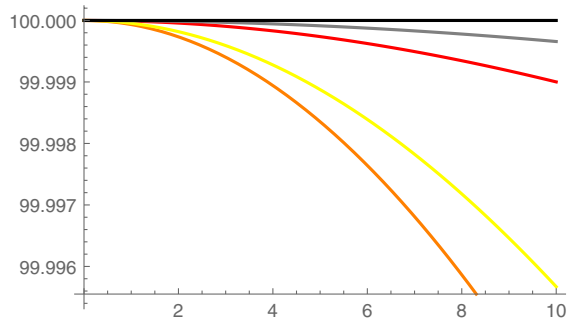

Fig. 4. Percentage similitude of the optical paths (PSOP). Black PSOP curve is for a stigmatic lens. Gray line is the sum of each optical path of Eq. (1). Red, orange, and yellow curves represent the PSOP curves for wavelengths $\lambda_1, \lambda_2, \lambda_3$, respectively.

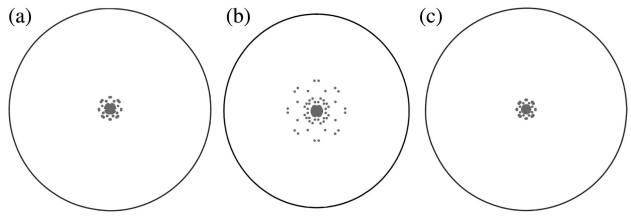

Fig. 5. Single-spot diagrams for the three wavelengths λ_1, λ_2, and λ_3. Black circles correspond to the Airy disks. For all the wavelengths, the spot images are inside the Airy disks.

system, we have computed the percentage similitude of the optical paths (PSOP). The PSOP measures how similar is the optical path of a non-axial ray with the optical path of the axial ray. We have

$$\left(1-\left|\frac{\text{LSH of Eq.(1)}-\text{RSHof Eq.(1)}}{\text{LSH of Eq.(1)}}\right|\right)\times 100\%, \quad \textbf{(8)}$$

where the term inside the absolute value is the normalized optical path difference (NOPD) between an axial ray and a non-axial ray.

In Fig. 4, we present the PSOP curves of interest. Black line corresponds to the stigmatic lens of Ref. [10] with the same data configuration of this example and with the refraction index given by $n=(n_1+n_2+n_3)/3$. In gray is the curve corresponding to the sum of each optical path of Eq. (1). The red, orange, and yellow curves represent wavelengths λ_1, λ_2, and λ_3, respectively.

The average results for 500 non-axial rays for the three wavelengths evaluating Eq. (5) is 99.9981%, and the result for the solution of the nonlinear system of Eqs. (1) and (4) is 99.99999%. Clearly the results of the nonlinear system are slightly better than those predicted by Eq. (5). However, for practical proposes, the shape designed with the simplified relation (5) is accurate enough.

The spot diagrams for the three wavelengths are depicted in Fig. 5. The black circles correspond to the respective Airy disks; thus, the spherochromatic singlet lens is diffraction limited. The radii of Airy disks for the three wavelengths are $r_1=0.003644$ nm, $r_2=0.002965$ nm, and $r_3=0.0041$ nm, and the radii of the image spots are $s_1=0.00017$ nm, $s_2=0.001065$ nm, and $s_3=0.00045$ nm. Both exact and simplified solutions give spot diagrams inside the Airy disk for the three wavelengths.

4. DISCUSSION AND CONCLUSION

In conclusion, we have introduced an analytical procedure to shape the output surface of a lens free of spherical and chromatic aberration. We derived the exact nonlinear system of algebraic equations and provided a very accurate simplified model that can be solved in closed form. The expressions can be applied for an arbitrary number of wavelengths. In the process, we have refuted the old paradigm introduced by Newton, which says that spherochromatic aberration can be not be reduced using a single lens.

Although for brevity only one example was included, the model is robust enough to design singlet lenses with a wide range of parameters, including different central thicknesses, source and object distances, and different wavelengths. It is important to remark that although Eq. (5) is analytically correct, it is hard to evaluate numerically when the refractive indices are very separated, for instance, $n_1=7$, $n_2=5$, and $n_3=2$. Fortunately, this situation is almost impossible to find in practical applications and optical materials where the change in the refraction index with respect to the wavelength is small.

Equation (5) seems to be cumbersome to evaluate because of its length, but actually it is just a simple evaluation. It was obtained using only algebra and the most fundamental principles in geometrical optics: the Snell law and the Fermat principle. The method presented looks very similar to the simultaneous multiple surfaces method (SMS), in that both use the one-to-one relation of the refraction points of every ray for each wavelength. The fundamental difference is that the presented method is analytical, while SMS is a numeric interpolation [18].

Finally, we want to remark that the problem proposed and solved in this paper is essentially the generalization of the problem mentioned by Christian Huygens in the preface and sixth chapter of his classical book *Traité de la lumière* [7]. The original problem expressed in Huygens's perspective is what the shape of a glass (lens) must be in order for it to collect the rays of one wavelength when one of the surfaces is given. In Ref. [10], we solved the original problem for one wavelength. In this paper, we present the solution for the case when the first surface is flat and for three different wavelengths. If we take $n_1=n_2=n_3$, Eq. (5) converges to the solution proposed in Ref. [10] when the first surface is flat and the spot diagram tends to be a single point.

Funding. Consejo Nacional de Ciencia y Tecnología (APN2016-3140).

Acknowledgment. We acknowledge support from Tecnológico de Monterrey.

Disclosures. The authors declare no conflicts of interest.

REFERENCES

1. M. Bass, *Handbook of Optics, Volume I: Fundamentals, Techniques, and Design* (McGraw-Hill, Inc., 1995).

2. H. Sun, *Lens Design: A Practical Guide* (CRC Press, 2016).
3. B. Braunecker, R. Hentschel, and H. J. Tiziani, *Advanced Optics Using Aspherical Elements* (SPIE Press, 2008), Vol. **173**.
4. I. Newton, *Opticks, or, a Treatise of the Reflections, Refractions, Inflections & Colours of Light* (Courier Corporation, 1979).
5. M. Daumas, *Scientific Instruments of the Seventeenth and Eighteenth Centuries and Their Makers, London (UK)* (Batsford, 1972).
6. G. J. Toomer, *Diocles, On Burning Mirrors: The Arabic Translation of the Lost Greek Original* (Springer Science & Business Media, 2012), Vol. **1**.
7. C. Huygens, *Traité de la lumière* (Macmillan, 1920).
8. F. J. Dijksterhuis, *Lenses and Waves: Christiaan Huygens and the Mathematical Science of Optics in the Seventeenth Century* (Springer Science & Business Media, 2004), Vol. **9**.
9. W. P. McCray, *Stargazer: the Life and Times of the Telescope* (2006).
10. R. G. González-Acuña and H. A. Chaparro-Romo, "General formula for bi-aspheric singlet lens design free of spherical aberration," Appl. Opt. **57**, 9341–9345 (2018).
11. G. Schulz, "Achromatic and sharp real imaging of a point by a single aspheric lens," Appl. Opt. **22**, 3242–3248 (1983).
12. F. Duerr, P. Bentez, J. C. Minano, Y. Meuret, and H. Thienpont, "Analytic design method for optimal imaging: coupling three ray sets using two free-form lens profiles," Opt. Express **20**, 5576–5585 (2012).
13. J. Chaves, *Introduction to Nonimaging Optics*, 2nd ed. (CRC Press, 2016).
14. J. Nagar, S. Campbell, and D. Werner, "Apochromatic singlets enabled by metasurface-augmented grin lenses," Optica **5**, 99–102 (2018).
15. R. G. González-Acuña and J. C. Guitiérrez-Vega, "Generalization of the axicon shape: the gaxicon," J. Opt. Soc. Am. A **35**, 1915–1918 (2018).
16. R. G. González-Acuña, H. A. Chaparro-Romo, and J. C. Gutiérrez-Vega, "General formula to design freeform singlet free of spherical aberration and astigmatism," Appl. Opt. **58**, 1010–1015 (2019).
17. R. G. González-Acuña, M. Avendaño-Alejo, and J. C. Gutiérrez-Vega, "Singlet lens for generating aberration-free patterns on deformed surfaces," J. Opt. Soc. Am. A **36**, 925–929 (2019).
18. O. Dross, R. Mohedano, P. Benitez, J. C. Minano, J. Chaves, J. Blen, M. Hernandez, and F. Munoz, "Review of SMS design methods and real-world applications," Proc. SPIE **5529**, 35–48 (2004).